Scientia Iranica B (2014) 21(6), 1861–1869

Sharif University of Technology
Scientia Iranica
Transactions B: Mechanical Engineering
www.scientiairanica.com

Synthesis of robust PID controller for controlling a single input single output system using quantitative feedback theory technique

M.R. Gharib* **and M. Moavenian**

Department of Mechanical Engineering, Ferdowsi University of Mashhad, Mashhad, Iran.

Received 27 December 2011; received in revised form 22 January 2014; accepted 17 March 2014

KEYWORDS
Quantitative Feedback Theory (QFT);
Rotary missile;
Nonlinear equations;
Robust PID.

Abstract. In this paper, the modeling and control of a rotary missile that uses the proportional navigation law is proposed, applying the Quantitative Feedback Theory (QFT) technique. The dynamics of a missile are highly uncertain; thus, application of robust control methods for high precise control of missiles is inevitable. In the modeling section, a new coordinate system has been introduced, which simplifies analysis of rotary missile dynamics equations. In the controlling part, application of the QFT method leads to the design of a robust PID controller for the highly uncertain dynamics of a missile. Since missile dynamics have multivariable nonlinear transfer functions, in order to apply the QFT technique, these functions are converted to a family of linear time invariant processes with uncertainty. Next, in the loop shaping phase, an optimal robust PID controller for the linear process is designed. Lastly, analysis of the design procedure shows that the robust PID controller is superior to the commonly used PID scheme and multiple sliding surface schemes, in terms of both tracking accuracy and robustness.

1. Introduction

Closed loop controlled missiles are designed, taking into consideration that they do not rotate around the longitudinal axis [1-8]. In order to control these missiles, we must control yaw and pitch channels independently. For analyzing the dynamics of a missile, both earth-fixed and body coordinate systems are normally employed. But, in this paper, a new coordinate system has been introduced which results in simplification of the dynamic modeling analysis, and obtains a linear uncertain SISO dynamic model for the missile. The main difference between controlling a Multiple-Input Multiple-Output (MIMO) system and a Single-Input Single-Output (SISO) system is in the process of assessing and compensating the interactions in the system degrees of freedom [9,10].

In summary, one can say that it is a complicated issue to implement an established SISO system control model on a MIMO system, because of extensive computational load.

The advantage of QFT, with respect to other robust control techniques such as H_∞ [11-16], is that their design is based on the magnitude of transfer function in the frequency domain. However, design of QFT [17-26] is not only concerned with the aforementioned subject, but is also able to take into account phase information. The unique feature of QFT is that the performance specifications are expressed as bounds on frequency-response loop shapes in such a way that the satisfaction of these bounds implies a corresponding approximate closed-loop satisfaction

*. *Corresponding author. Tel.: +98 915 322 8499*
E-mail address: Mech_gharib@yahoo.com (M.R. Gharib)

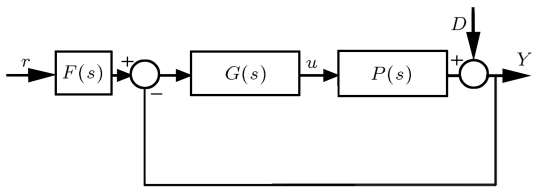

Figure 1. Two-degree-of-freedom feedback system.

of time-domain response bounds for given classes of inputs and for all uncertainty in a given compact set.

Consider the feedback system shown in diagram of Figure 1. This system has a two-degree-of-freedom structure. In this diagram, $p(s)$ is an uncertain plant belonging to a set that is $p(s) \in \{p(s,\alpha); \alpha \in p\}$, where α is the vector of uncertain parameters. $P(s)$ and $G(s)$ are plants with an uncertainty structure and a fixed structure feedback controller, respectively. $F(s)$ is the pre-filter and $D(s)$ is the disturbance at the plant output.

2. Missile's model

To obtain the missile's dynamic model, three coordinate systems are defined.

The origin of the earth-fixed coordinate system is located at the missile's launch point [1,3].

The origin of the body coordinate system is assumed to be at the missile center of gravity. The X_B-axis of the body coordinate system points in the direction of the missile nose, the Y_B-axis points in the starboard direction, and the Z_B-axis completes the right-handed triad [3].

A new method for dynamic modeling of a rotary missile, based on suggesting a new irrotational body coordinate system, has been introduced, which eliminates the interaction between pitch and yaw channels. This coordinates system is defined as below:

The body irrotational coordinates system is assumed to be at the missile's center of gravity. The X_S-axis system points in the direction of the missile nose, the Y_S-axis in the yaw channel, and the Z_S-axis in the pitch channel.

The body coordinate system and the inertial coordinate systems are used to derive the equations of motion. These coordinate systems are illustrated in Figure 2.

Based on Newton's second rule, we know that the force is equal to changes in the vector of momentum [1]:

$$F = F^S = \begin{bmatrix} F_X & F_Y & F_Z \end{bmatrix}^T, \tag{1}$$

$$\omega = \omega_{IS}^S = \begin{bmatrix} p & q & r \end{bmatrix}^T, \tag{2}$$

$$V = V^s = \begin{bmatrix} u & v & w \end{bmatrix}^T, \tag{3}$$

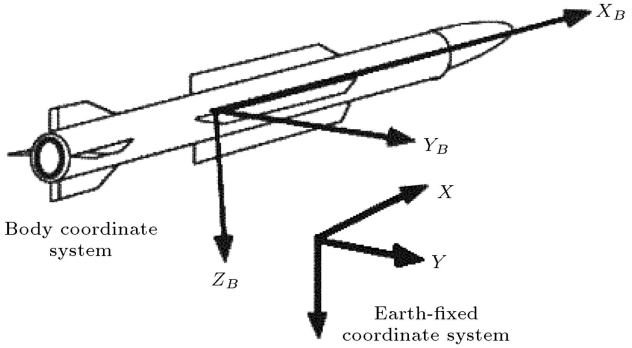

Figure 2. Missile's coordinate systems [3].

$$\begin{cases} F_x = \dot{M}u + M(\dot{u} + qw - rv) \\ F_y = \dot{M}v + M(\dot{v} + ru - pw) \\ F_z = \dot{M}w + M(\dot{w} + pv - qu) \end{cases} \tag{4}$$

where u, v and w are the speed components measured in the missile body axes system, and p, q and r are the components of the body angular velocity [1,3].

Consider that $H^S = I\omega_{IB}^S$ and I is the moment of inertia of the missile in the body irrotational coordinates system. By reason of symmetry around the missile longitudinal axis, I matrix is $I = \text{diag}\{I_{xx}, I_{zz} I_{zz}\}$. Also, ω_{IB}^S is the angular velocity vector (that rotates with the body coordinate system), which is expressed in terms of frame $\{S\}$.

If the angular velocity around the longitudinal axis is s, then:

$$\omega_{IB}^S = \omega_{IS}^S + \begin{bmatrix} s & 0 & 0 \end{bmatrix}^T = \begin{bmatrix} s+p & q & r \end{bmatrix}^T. \tag{5}$$

So, by applying Eq. (5) and the definition of H^S:

$$H^S = I\omega_{IB}^S = \begin{bmatrix} I_{xx}p + I_{xx}s & I_{zz}q & I_{zz}r \end{bmatrix}. \tag{6}$$

Using Eq. (6), Coriolis and Newton's rules, and assuming $\tau^2 = \begin{bmatrix} l & m & n \end{bmatrix}^T$ (where τ is a vector of moment), yields [1]:

$$\begin{cases} l = \dot{I}_{xx}(p+s) + I_{xx}(\dot{p} + \dot{s}) \\ m = \dot{I}_{xx}q + I_{zz}\dot{q} + (I_{xx} - I_{zz})qr + I_{xx}sr \\ n = \dot{I}_{xx}r + I_{zz}\dot{r} - (I_{zz} - I_{xx})pq - I_{xx}sq \end{cases} \tag{7}$$

2.1. Linearization of model

The state vector is defined as [1,5]:

$$x = \begin{bmatrix} u & v & w & p & q & r \end{bmatrix}^T.$$

Angle of attack (α) and angle of sideslip (β) can be defined as follows:

$$\alpha = \tan^{-1}\left(\frac{v}{u}\right), \qquad \beta = \tan^{-1}\left(\frac{w}{u}\right). \tag{8}$$

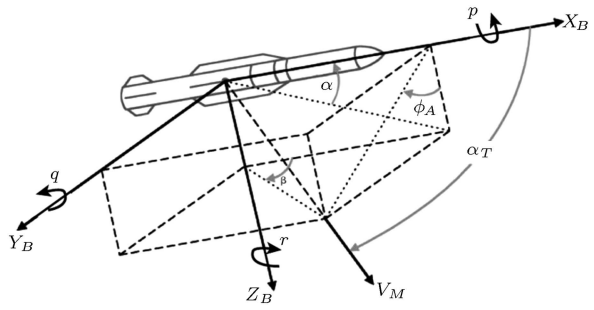

Figure 3. Motion variable notations.

Aerodynamics force and moment are functions of the angles of attack (α), sideslip, fins ($\delta p, \delta d$) and angular velocity (p, q, r) (Figure 3) [1].

Since the missile has one movable fin, as a result of rotation, it can be supposed that the missile has two movable fins, separately, in y, z directions in the body irrotational coordinate system.

The equivalent fin in the Y-axis direction is named the lifter fin, and δp is a small deviation of it. The second fin is named the rotating fin and δd is a small deviation of that.

For linearization, aerodynamics force and moment are assumed linear functions.

The translational and rotational dynamics of the missile are described by the following six nonlinear differential equations:

$$\begin{aligned}
\dot{x}_1 =& -\left(\dot{M}_0/M_0\right)x_1 - x_2x_6 - x_3x_5 \\
&+ (1/M_0)\Big\{\tan^{-1}(x_3/x_1)C_{x\alpha} \\
&+ \tan^{-1}(x_2/x_1)C_{x\beta} + C_{x\delta p}\delta p + C_{x\delta d}\delta d \\
&+ C_{yq}x_5 + F_{x\text{prop}}\Big\}, \\
\dot{x}_2 =& -\left(\dot{M}_0/M_0\right)x_2 - x_1x_6 - x_3x_4 \\
&+ (1/M_0)\big\{\tan^{-1}(x_3/x_1)C_{y\alpha} \\
&+ \tan^{-1}(x_2/x_1)C_{y\beta} + C_{y\delta p}\delta p + C_{y\delta d}\delta d \\
&+ C_{yq}x_5 + F_{y\text{prop}}\big\}, \\
\dot{x}_3 =& -\left(\dot{M}_0/M_0\right)x_3 - x_1x_5 - x_2x_4 \\
&+ (1/M_0)\big\{\tan^{-1}(x_3/x_1)C_{z\alpha} \\
&+ \tan^{-1}(x_3/x_1)C_{z\beta} + C_{z\delta p}\delta p \\
&+ C_{z\delta d}\delta d + C_{zq}x_5 + F_{z\text{prop}}\big\}, \\
\dot{x}_4 =& -\left(\dot{I}_{xx_0}/I_{xx_0}\right)x_4 - \left(\dot{I}_{xx_0}/I_{xx_0}\right)s \\
&+ (1/I_{xx_0})\big\{\tan^{-1}(x_3/x_1)C_{l\beta} + C_{l\delta p}\delta p \\
&+ C_{l\delta d}\delta d + C_{lp}x_4 + l_{\text{prop}}\big\}, \\
\dot{x}_5 =& -\left(\dot{I}_{zz_0}/I_{zz_0}\right)x_5 + I'x_4x_6 - (I_{xx_0}s/I_{zz_0})x_6 \\
&+ (1/I_{zz_0})\big\{\tan^{-1}(x_3/x_1)C_{m\alpha} \\
&+ \tan^{-1}(x_2/x_1)C_{m\beta} + C_{m\delta p}\delta p + C_{m\delta d}\delta d \\
&+ C_{mr}x_5 + m_{\text{prop}}\big\}, \\
\dot{x}_6 =& -\left(\dot{I}_{zz_0}/I_{zz_0}\right)x_6 + I'x_4x_5 - (I_{xx_0}s/I_{zz_0})x_5 \\
&+ (1/I_{zz_0})\big\{\tan^{-1}(x_3/x_1)C_{n\alpha} \\
&+ \tan^{-1}(x_2/x_1)C_{n\beta} + C_{n\delta p}\delta p + C_{n\delta d}\delta d \\
&+ C_{nr}x_6 + n_{\text{prop}}\big\}, \qquad (9)
\end{aligned}$$

where $I' = (I_{zz_0} - I_{xx_0})/I_{zz_0}$ and prop index are related to forces and moments produced from combustion of the missile, and C coefficients are aerodynamic factors of the missile. The result of linearizing Eq. (9) in the operating point (V_0, ω_0), when $u = u_0 + \delta u$, is given by [4], as follows:

$$\begin{aligned}
\dot{\delta X} =& \begin{bmatrix} A1 & A2 & A3 & 0 & 0 & 0 \\ 0 & A4 & 0 & 0 & 0 & A5 \\ 0 & 0 & A6 & 0 & A7 & 0 \\ 0 & 0 & 0 & A8 & 0 & 0 \\ 0 & 0 & A9 & 0 & A10 & A11 \\ 0 & A12 & 0 & 0 & A13 & A14 \end{bmatrix} \delta X \\
&+ \begin{bmatrix} B1 & B1 \\ 0 & B1 \\ B1 & 0 \\ 0 & 0 \\ B1 & 0 \\ 0 & B1 \end{bmatrix} \delta u, \qquad (10)
\end{aligned}$$

A1	**A2**	**A3**
$-\frac{\dot{M}_0}{M_0}$	$\frac{C_{x\beta}}{u_0 M_0}$	$\frac{C_{x\alpha}}{u_0 M_0}$
A4	**A5**	**A6**
$-\frac{\dot{M}_0}{M_0} + \frac{C_{y\beta}}{u_0 M_0}$	$u_0 + C_{yr}$	$-\frac{\dot{M}_0}{M_0} + \frac{C_{z\alpha}}{u_0 M_0}$
A7	**A8**	**A9**
$u_0 + C_{zq}$	$\frac{-\dot{I}_{xx_0} + C_{lp}}{I_{xx_0}}$	$\frac{C_{m\alpha}}{u_0 I_{zz_0}}$
A10	**A11**	**A12**
$\frac{-\dot{I}_{zz_0} + C_{mq}}{I_{zz_0}}$	$\frac{I_{xx_0} s}{I_{zz_0}}$	$\frac{C_{n\beta}}{u_0 I_{zz_0}}$
A13	**A14**	**B1**
$\frac{I_{xx_0} s}{I_{zz_0}}$	$\frac{-\dot{I}_{zz_0} + C_{nr}}{I_{zz_0}}$	$C_{X\delta p}$

The system outputs are (r, q).

According to the state space model, x_2 is related to x_6, x_3 is related to x_5. x_2 and x_6 states represent the yaw channel, while x_3 and x_5 states express the pitch channel in common missiles. The main system can be divided into two subsystems; yaw and pitch channels. x_1 and x_4 states have no effect on pitch and yaw channels, but the stability of these channels causes the stability of x_1 and x_4 states. The outputs of the system are the angular velocities of the missile (in the normal direction of the longitudinal axis).These angular velocities are related to pitch and yaw channels. By controlling the missile in these channels, a good performance will be resulted. In the irrotational body coordinate system, the only interaction between these channels is the term $(I_{xx_0}s/I_{zz_0})$. According to the physical shape of the missile, I_{zz_0} is approximately 100 times greater than I_{xx_0}. By ignoring the interaction between these channels, the state space of the pitch channel is:

$$y = \begin{bmatrix} 0 & 1 \end{bmatrix} \begin{bmatrix} x_2 \\ x_6 \end{bmatrix},$$

$$\begin{bmatrix} \dot{x}_2 \\ \dot{x}_6 \end{bmatrix} = \begin{bmatrix} -\frac{\dot{M}_0}{M_0} + \frac{C_{y\beta}}{u_0 M_0} & u_0 + c_{yr} \\ \frac{c_{n\beta}}{u_0 I_{zz_0}} & \frac{-\dot{I}_{zz_0} + c_{nr}}{I_{zz_0}} \end{bmatrix} \begin{bmatrix} x_2 \\ x_6 \end{bmatrix} + \begin{bmatrix} c_{y\delta d} \\ c_{n\delta d} \end{bmatrix} \delta d. \quad (11)$$

From state equations to transfer function. Consider the system described by state Eq. (11). The system's transfer function, $G(s)$, is $G(s) = C(sI - A)^{-1}B + D$.

According to the relation between aerodynamic coefficients in yaw and pitch channels, in these channels, transfer functions between output (angle of fin) and input (angular velocity) are identical and only differ in the sign. So, the designed controller for one channel can be used for another channel by changing its sign.

A missile is a guidable flying machine with variable transfer functions. This means that by changing the speed, flying height and mass, and the parameters of flying, the transfer function will change. Variation of speed is especially important, which causes variation in the aerodynamic coefficients. So, by applying Eq. (12), shown in Box I, and using a servo motor at four different Machspeeds, the missile transfer functions will be obtained.

For the model of the pitch channel missile:

$$P(s) = \frac{as + b}{cs^3 + ds^2 + es + 1},$$

$$a = \begin{bmatrix} 0.27 & 1.7 \end{bmatrix}, \qquad b = \begin{bmatrix} 0.41 & 1.7 \end{bmatrix},$$

$$c = \begin{bmatrix} 1.4 \times 10^{-6} & 1.47 \times 10^{-5} \end{bmatrix},$$

$$d = \begin{bmatrix} 0.0016 & 0.0073 \end{bmatrix}, \qquad e = \begin{bmatrix} 0.31 & 0.91 \end{bmatrix}. \quad (13)$$

3. Quantitative Feedback Theory (QFT)

There are many practical systems that have high uncertainty in open-loop transfer functions, which makes it very difficult to have suitable stability margins and proper performance in command following problems in the closed-loop system. Therefore, a single fixed controller in such systems is found amongst the "robust control" family.

Quantitative Feedback Theory (QFT) is a robust feedback control-system design technique initially introduced by Horowitz (1963, 1979), which allows direct design to closed-loop robust performance and stability specifications. Since then, this technique has been further developed by him and others [9-21].

Simply, the QFT controller design method can be summarized as follows.

In parametric uncertain systems, we must first generate plant templates prior to the QFT design (at a fixed frequency, the plant's frequency response set is called a *template*). Given the plant templates, QFT converts closed loop magnitude specifications into magnitude constraints on a nominal open-loop function (these are called QFT *bounds*). A nominal open loop function is then designed to simultaneously satisfy its constraints, as well as to achieve nominal closed loop stability. In a two-degree-of-freedom design, a pre-filter will be designed after the loop is closed (i.e., after the controller has been designed) [12].

4. Optimal controller design

QFT tunes the G controller with the objective of reducing control bandwidth while maintaining robust performance. A desired modification in small frequency bands is transparent using QFT's open-loop tuning. The bandwidth control point of view was introduced

$$\frac{\delta r}{\delta d} = \frac{C_{n\delta d}s + \left(\frac{C_{n\delta d}\dot{M}_0}{M_0} + \frac{C_{n\beta}C_{y\delta d}}{u_0 I_{zzo}} - \frac{C_{n\delta d}C_{y\beta}}{u_0 M_0}\right)}{s^2 + \left(\frac{\dot{M}_0}{M_0} - \frac{C_{y\beta}}{u_0 M_0} + \frac{\dot{I}_{zzo}}{I_{zzo}} - \frac{C_{nr}}{I_{zzo}}\right)s + \left(\frac{\dot{M}_0 \dot{I}_{zzo}}{M_0 I_{zzo}} + \frac{C_{y\beta}C_{nr}}{u_0 M_o I_{zzo}} - \frac{C_{y\beta}\dot{I}_{zzo}}{u_0 M_o I_{zzo}} - \frac{\dot{M}_0 C_{nr}}{M_0 I_{zzo}} + \frac{C_{n\beta}}{I_{zzo}} - \frac{C_{n\beta}C_{yr}}{u_0 I_{zzo}}\right)}. \quad (12)$$

Box I

by Chait and Hollot (1990) [22-26]. A key limitation of the mentioned procedure is that the poles of T are fixed with only the zeros taken as optimization variables. So, in the second step, we optimize the denominator coefficients, where the cost function is the quadratic sum of Euclidean distance between the open-loop response and the bounds in the Nichols plane. This minimization tries to reach the optimal loop-shaping defined by Zhang et al. [27] and Horowitz and Sidi [31].

In the design stage (loop-shaping), the controller, $G_C(s)$, is synthesized by adding poles and zeros until the nominal loop, defined as $L_0 = G_0 G_C$, lies near its bounds. An optimal controller will be obtained if it meets its bounds while it has minimum high frequency gain. So, application of this method to obtain the minimum gain of the controller is employed here. Hence, there is no need to be concerned about saturation. As a comprehensive optimal QFT controller design is not the main contribution of this paper, it will be dealt with in future research.

5. PID controller

A realistic definition of optimum in LTI systems is minimization of the high-frequency loop gain, k, while satisfying performance bounds. This gain affects the high-frequency response, since $\lim_{\omega\to\infty}[L(j\omega)] = K(j\omega)^{-\lambda}$, where λ is the excess of poles over zeros assigned to $L(j\omega)$. Thus, only the gain, K, has a significant effect on the high-frequency response, and the effect of the other parameter uncertainty is negligible. It has been shown that if the optimum, $L_0(j\omega)$ exists, then, it lies on the performance bounds at all ω_i, and it is unique [14]. In this part, we will introduce a simple algorithm for designing an optimal PID controller. A PID controller has a transfer function;

$$G_{\text{pid}}(s) = k_p + \frac{k_i}{s} + k_d s. \tag{14}$$

Three used terms in Eq. (14) are defined as: k_p (proportional gain), k_i (integral gain) and k_d (derivative gain). Our method for designing an optimal PID controller is based on designing a specific lead-lag compensator, which transforms into a PID controller under special conditions.

Consider the closed-loop system in Figure 1 in which $G(s)$ is a below lag-lead compensator:

$$G(s) = Ka \times \frac{s + \frac{1}{T_1}}{s + \frac{a}{T_1}} \times \frac{s + \frac{1}{T_2}}{s + \frac{1}{aT_2}}. \tag{15}$$

In order to achieve a PID controller, let us move a towards infinity value, so, we will have:

$$\lim_{a\to\infty} G(s) = \frac{KT_1}{s}\left[\left(s + \frac{1}{T_1}\right) \times \left(s + \frac{1}{T_2}\right)\right], \tag{16}$$

$$\Rightarrow G(s) = KT_1\left(\frac{1}{T_1} + \frac{1}{T_2}\right) + \left(\frac{K}{T_2}\right)\frac{1}{s} + KT_1 s. \tag{17}$$

So, we have a PID controller which is defined by:

$$k_p = K\left(\frac{T_1 + T_2}{T_2}\right), \qquad k_i = \frac{K}{T_2}, \qquad k_d = KT_1. \tag{18}$$

Up to now, two real poles of the lag-lead compensator have been specified: one located in infinity and the other in the origin. In order to define the PID controller in the next step of this algorithm, we must specify the gain, K, and the situation of two zeros of $G(s)$. But, as mentioned before, the optimum, $L_0(j\omega)$, must lie exactly on its performance bounds at all frequency values (ω_i). Therefore, in the last phase of this algorithm, the suitable location of these two zeros can be achieved by a trial and error procedure using the Interactive Design Environment (IDE) of QFT [21].

Under special circumstances, using only one zero in the loop shaping phase will result in the PI controller (considering the lag-compensator), and the PD controller will be resulted by elimination of the pole in the origin.

6. Design of robust controller for the missile

The objective of this part is to synthesize a suitable controller and pre-filter, such that, first, the closed loop system is stable and, second, it can track the desired inputs.

1. Stability margin:

$$\left|\frac{P(j\omega)G(j\omega)}{1 + P(j\omega)G(j\omega)}\right| < 1.2. \tag{19}$$

2. The tracking specification is overshoot (= 5%) and the settling time (= 0.005 s) for all plant uncertainty, which can be described with a second order system:

$$|\alpha(j\omega_i)| \le |T(j\omega_i)| \le |\beta(j\omega_i)|, \tag{20}$$

where $\alpha(j\omega_i)$ and $\beta(j\omega_i)$ are lower bound and upper bounds, respectively, and $T(j\omega_i)$ is the input-output relation from input $R(s)$ to output $Y(s)$.

At the first step, the plant uncertainty must be defined (template). Thus, the boundaries of the plant templates have been computed and are shown in Figure 4. Next, having plant templates and required performance specifications, we can compute robust performance bounds, which are shown in Figure 5. Then, by having robust performance bounds in the loop-shaping phase of the design, by applying the algorithm developed in part 4, we can design a suitable

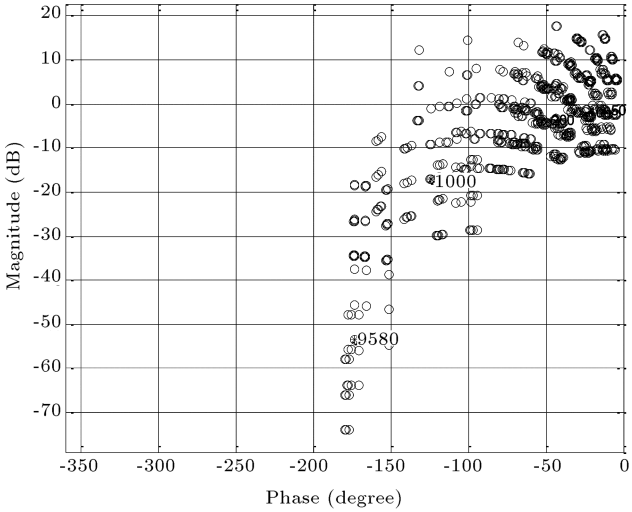

Figure 4. Plant uncertainty templates.

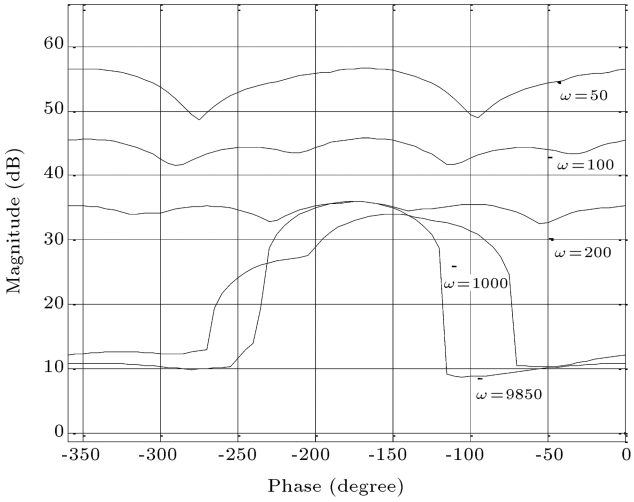

Figure 5. Intersection bounds.

PID controller. Figures 6 and 7 depict the loop and prefilter shaping of the open loop transfer function. In the loop shaping design, one can observe that the nominal plants lie on their performance bounds, which confirms the optimal design of robust controllers. According to the loop shaping phase, optimal robust PID controllers are as follows:

$$G(s)_{\text{PID}} = 169 + 0.17s + \frac{2.15 \times 10^4}{s}, \tag{21}$$

$$F(s) = \left(\frac{s}{3596} + 1\right)^{-1} \left(\frac{s}{4782} + 1\right)^{-1}. \tag{22}$$

7. Analysis of design

In this part, the robust stability of the closed-loop system and, also, tracking specifications in both time and frequency domains is investigated for all considered uncertainty of the missile dynamics. Frequency domain stability is shown in Figure 8.

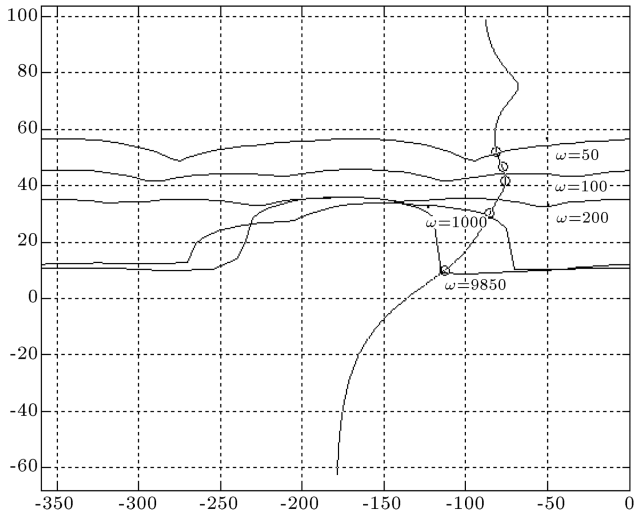

Figure 6. Loop shaping of open-loop system.

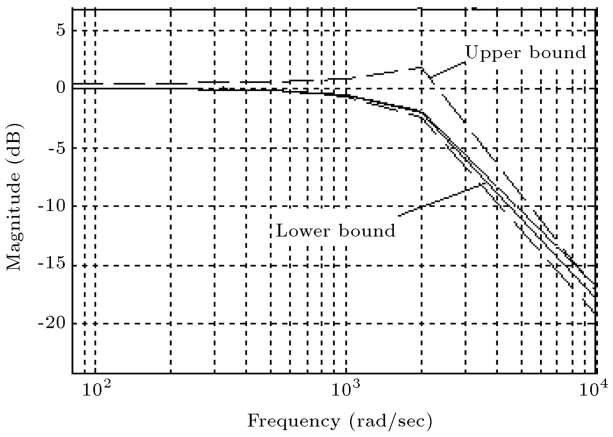

Figure 7. Prefilter shaping of open-loop system.

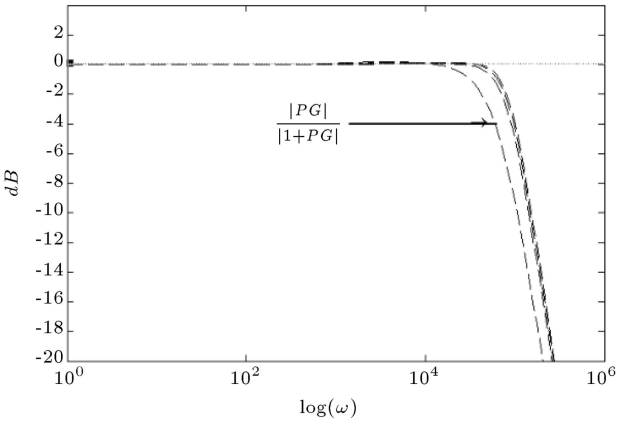

Figure 8. Robust stability of closed-loop system.

The frequency-domain closed-loop response is shown in Figure 9 and, consequently, the time-domain closed-loop response is shown in Figure 10. Hence, according to linear simulation, the missile has robust stability and can also satisfy tracking specifications.

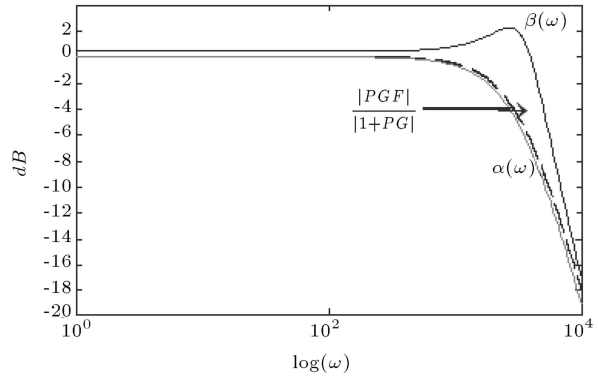

Figure 9. Closed-loop frequency response.

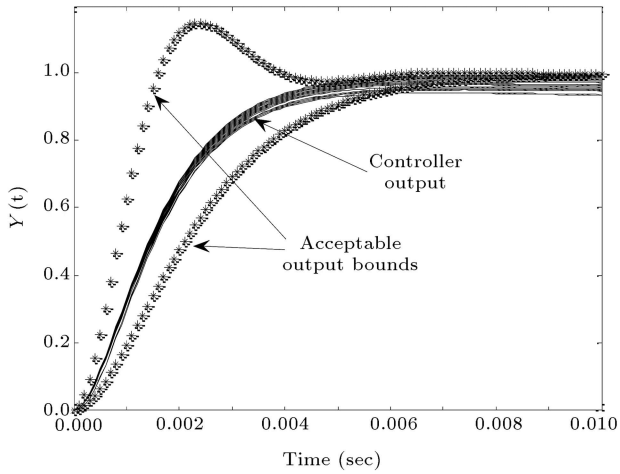

Figure 10. Unit step response.

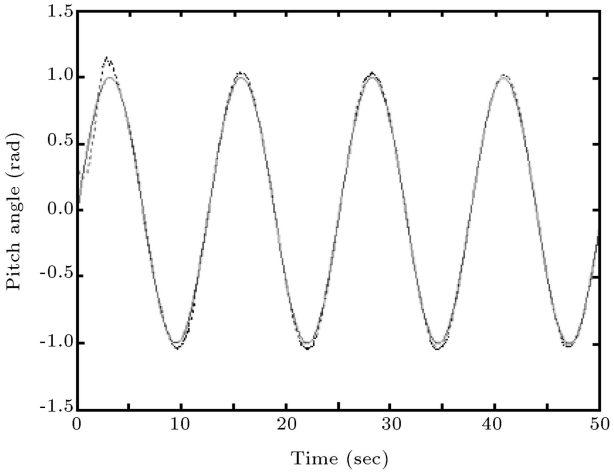

Figure 11. Tracking performance of pitch angle $\theta(t)$ to the commanded pitch angle $\theta_d(t)$ (solid line: $\theta_d(t)$, dotted line: $\theta(t)$) using MSS [32].

7.1. Comparison of QFT controller with MSS control approach in control of pitch channel

Angular tracking responses were used to evaluate the control performance of the missile pitch channel. Figures 11 and 12 show simulations of angular tracking responses related to MSS [32] and QFT applied in this work, respectively.

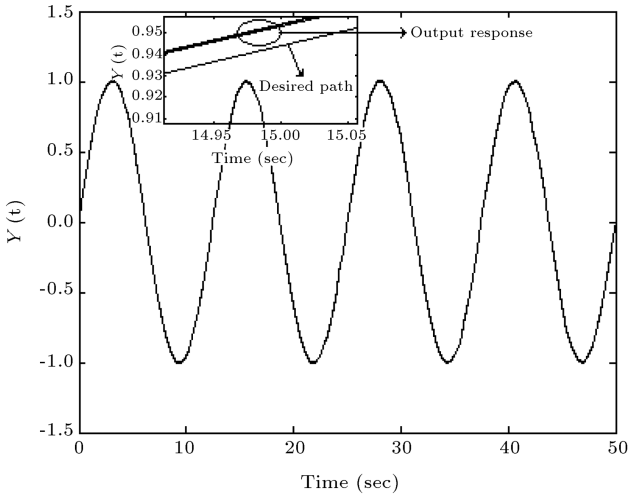

Figure 12. Tracking performance of pitch angle using QFT.

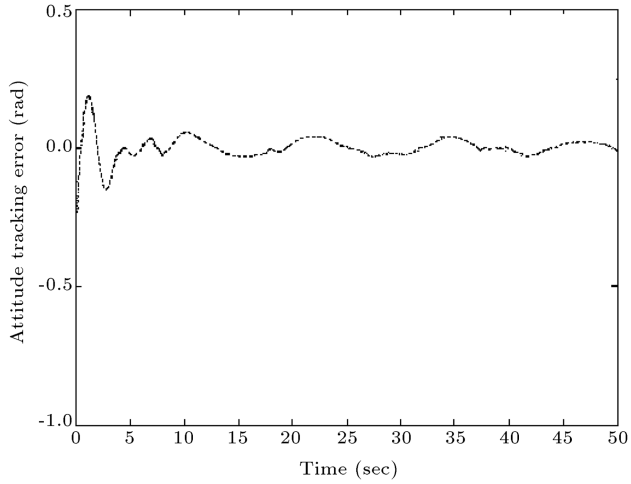

Figure 13. Tracking errors versus time of pitch angle using MSS [29].

Comparison of the MSS [32] method with the QFT controller, regarding angular tracking errors, demonstrates that the QFT technique, in the presence of all uncertainties, suggests a controller which has a better control performance, with respect to maximum and integral absolute errors (Figures 13 and 14).

8. Conclusion

In this article, after achieving the dynamic model of the missile, QFT is introduced as a robust controlling design method, and application of the proposed third coordinate system simplified the dynamic modeling of the missile. This caused the nonlinear MIMO system to be converted to a linear SISO system. In order to compensate the uncertainties involved, a family of linear uncertain SISO systems is introduced. Then,

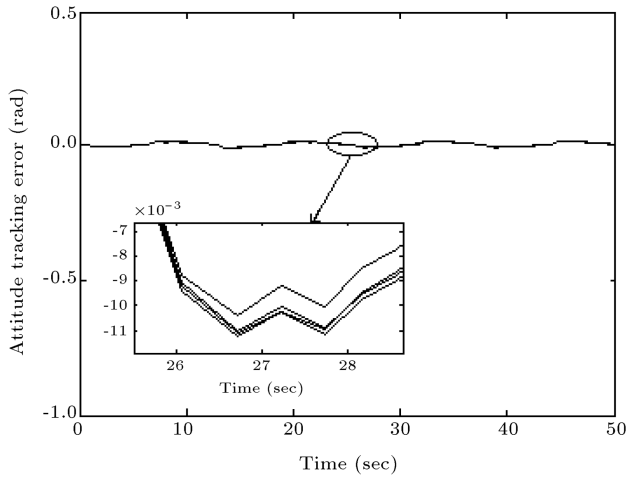

Figure 14. Tracking errors versus time of pitch angle using QFT.

an optimal robust PID controller for the linear process is designed. Finally, the results obtained from the controller output designed using the QFT method are compared with reported results of a multiple sliding surface controller designed by "Lu, Zhao. et al." [32]. It is shown that the QFT technique suggests a controller with a better control performance.

Nomenclature

α	Angle of attack (°)
β	Angle of sideslip (°)
δp	Small deviation of lift fin
δd	Small deviation of rotating fin
$\alpha(S)$	Uncertain parameters vector
$\omega_x, \omega_y, \omega_z$	Angular velocity components (rad/s)
δ_α	Deflection angle in the pitch plane (°)
δ_β	Deflection angle in the yaw plane (°)
k_d	Derivative gain
δ	Fractional derivative
λ	Fractional integration
$P(s,\alpha)$	Uncertain plant
X_b, Y_b, Z_b	Body coordinate
$G(s)$	Compensator
F_x, F_y, F_z	Components of total forces acting on missile (N)
M_x, M_y, M_z	Components of total moments acting on missile (N m)
$D(s)$	Disturbance
C_x	Drag coefficient
X_g, Y_g, Z_g	Ground coordinate
k_i	Integral gain
u, v, w	Velocity components (m/s)
S	Laplace variable
C_z	Lateral coefficient
C_y	Lift coefficient
I_x, I_y, I_z	Moment of inertia components (kg m^2/s)
$F(s)$	Pre-filter
k_p	Proportional gain
r	Reference signal
M	The mass of missile (kg)

References

1. Blacklock, J.H., *Automatic Control of Aircraft and Missile*, 2nd Ed., John Wiley & Sons Publition, New York, Chaps. 1, 4, 7, 8 (1991).
2. Zarchan, P. "Proportional navigation and weaving targets", *Journal of Guidance, Control and Dynamics*, **18**(5), pp. 969-974 (1995).
3. Menona, P.K. and Ohlmeyer, E.J. "Integrated design of agile missile guidance and autopilot systems", *Control Engineering Practice Journal*, **9**(10), pp. 1095-1106 (2001).
4. Seraj, H. and Masominya, M.A. "Modeling and control of a rotational missile", *ICEE Conference*, Isfahan, pp. 10- 17, Printed in Farsi (2000).
5. Faruqi, F.A. and Lan Vu, T., *Mathematical Models for a Missile Autopilot Design*, 1st Ed., DSTO Systems Sciences Laboratory Publication, Edinburgh, South Australia (2002).
6. Lidan, X., Ke'nan, Z., Wanchun, Ch. and Xingliang, Y. "Optimal control and output feedback considerations for missile with blended aero-fin and lateral impulsive thrust", *Chinese Journal of Aeronautics*, **23**, pp. 401-408 (2010).
7. Ahmeda, W.M. and Quan, Q. "Robust hybrid control for ballistic missile longitudinal autopilot", *Chinese Journal of Aeronautics*, **24**, pp. 777-788 (2011).
8. Mingzhe, H., Xiaoling, L. and Guangren, D. "Adaptive block dynamic surface control for integrated missile guidance and autopilot", *Chinese Journal of Aeronautics*, **26**(3), pp. 741-750 (2013).
9. Gharib, M., Amiri Moghadam, A.A. and Moavenian, M. "Optimal controller design for two arm manipulators using quantitative feedback theory method", *24th International Symposium on Automation and Robotics in Construction*, India (2007).
10. Yaniv, O. "Automatic loop shaping of MIMO controllers satisfying sensitivity specifications", *ASME Journal of Dynamic Systems, Measurement, and Control*, **128**, pp. 463-471 (2006).
11. Kim, C.S. and Lee, K.W. "Robust control of robot manipulators using dynamic under parametric uncertainty", *International Journal of Innovative Compensators Computing, Information and Control*, **7**(7(B)), pp. 4129-4139 (2011).

12. Bi, Sh., Deng, M. and Inoue, A. "Operator based robust stability and tracking performance of MIMO nonlinear systems", *International Journal of Innovative Computing, Information and Control*, **5**(10(B)), pp. 3351-3358 (2009).
13. Tootoonchi, A.A., Gharib, M.R. and Farzaneh, Y. "A new approach to control of robot", *IEEE RAM*, pp. 649-654 (2008).
14. Fateh, M.M. "Robust control of electrical manipulators by joint acceleration", *International Journal of Innovative Computing, Information and Control*, **6**(12), pp. 5501-5511 (2010).
15. Moghadam, A., Gharib, M.R., Moavenian, M. and Torabi, K. "Modeling and control of a SCARA robot using quantitative feedback theory", *Proc. IMechE Part I: J. Systems and Control Engineering*, **223**(17), pp. 901-918 (2009).
16. Isidori, A., *Nonlinear Control Systems*, Berlin, Springer (1989).
17. Horowitz, I.M. "Survey of quantitative feedback theory", *Int. J. Control Journal*, **53**(2), pp. 255- 261 (1991).
18. Golubev, B. and Horowitz, I.M. "Plant rational transfer function approximation from input-output data", *International Journal of Control*, **36**(4), pp. 711-723 (1982).
19. Jayasuriya, S., Nwokah, O., Chait, Y. and Yaniv, O. "Quantitative feedback (QFT) design: Theory and applications", *American Control Conference Tutorial Workshop*, Seattle, Washington (June 19-20, 1995).
20. Yaniv, O. and Horowitz, I.M. "Quantitative feedback theory for uncertain MIMO plants", *International Journal of Control*, **43**, pp. 401-421 (1986).
21. Kerr, M.L., Jayasuriya, S. and Asokanthan, S.F. "Robust stability of sequential multi-input multi-output quantitative feedback theory designs", *ASME Journal of Dynamic Systems, Measurement, and Control*, **127**, pp. 250-256 (2005).
22. Zoloas, A.C. and Halikias, G.D. "Optimal design of PID controllers using the QFT method", *IEE Proc-Control Theory Appl*, **146**(6), pp. 585-589 (1999).
23. Lin, T.C., Kuo, M.J. and Hsu, C.H. "Robust adaptive tracking control of multivariable nonlinear systems based on interval type-2 fuzzy approach", *International Journal of Innovative Computing, Information and Control*, **6**(3(A)), pp. 941-963 (2010).
24. García-Sanz, M., Egaña, I. and Barreras, M. "Design of quantitative feedback theory non-diagonal controllers for use in uncertain multiple-input multiple-output systems", *IEEE Proceedings-Control Theory and Applications*, **152**(2), pp. 177-187 (2005).
25. Yang, S.H. "An improvement of QFT plant template generation for systems with affinely dependent parametric uncertainties", *Journal of the Franklin Institute*, **346**(7), pp. 663-675 (2009).
26. Wang, Y.F., Wang, D.H., Chai T.Y. and Zhang, Y.M. "Robust adaptive fuzzy tracking control with two errors of uncertain nonlinear systems", *International Journal of Innovative Computing, Information and Control*, **6**(12), pp. 5587-5597 (2010).
27. Zhang, Y., Liang, X., Yang, P., Chen, A. and Yuan, Z. "Modeling and control of nonlinear discrete-time systems based on compound neural networks", *Chinese Journal of Chemical Engineering*, **17**(3), pp. 454-459 (2009).
28. Yanou, A., Deng, M. and I.A. "A design method of extended generalized minimum variance control based on state space approach by using a genetic algorithm", *International Journal of Innovative Computing, Information and Control*, **7**(7(B)), pp. 4183-4195 (2011).
29. Chait, Y. and Hollot, C.V. "A comparison between H-infinity methods and QFT for a SISO plant with both parametric uncertainty and performance specifications", O.D.I Nwokah, Ed., *Recent Development in Quantitative Feedback Theory*, pp. 33-40 (1990).
30. Horowitz, I.M. "Optimum loop transfer function in single-loop minimum-phase feedback systems", *Int. J. Control*, **1**, pp. 97-113 (1973).
31. Horowitz, I.M. and Sidi, M. "Optimum synthesis of non-minimum phase feedback systems with plant uncertainty", *Int. J. Control*, **27**(3), pp. 361-384 (1978).
32. Lu, Zhao, Lin, Feng and Ying, Hao "Multiple sliding surface control for systems in nonlinear block controllable form", *Cybernetics and Systems: An International Journal*, **36**, pp. 513-526 (2005).

Biographies

Mohammad Reza Gharib was born in Mashhad, Iran, in 1981. He received BS and MS degrees in Mechanical Engineering, in 2004 and 2006, from Ferdowsi University of Mashhad, Iran, where he is currently pursuing his PhD degree. His current research interests include control theories, mainly focusing on Quantitative Feedback Theory and the dynamics of quadrotors.

Majid Moavenian received his Bachelor of Science in Mechanical Engineering from the University of Tabriz, Iran. He also earned his MSc and PhD Degrees in Mechanical Engineering from Aston University and University of Wales College Cardiff, respectively. Currently he is an associate professor at Ferdowsi University of Mashhad while his research interests are in the areas of system design and fault detection.